

# Exact Design of Band-Stop Microwave Filters\*

B. M. SCHIFFMAN†, MEMBER, IEEE, AND G. L. MATTHAEI†, MEMBER, IEEE

**Summary**—An exact method for the design of band-stop filters which adapts synthesis techniques due to Ozaki and Ishii is discussed. This method places no theoretical limit on the width of the stop-band, although, for practical reasons, different (but equivalent) circuit configurations are used for stop-bands of different widths. These configurations include a form having open-circuited shunt stubs separated by lengths of line; a second form using resonators which are separate from the main line but parallel to it, so that coupling takes place by way of fringing fields; and a third form in which the resonators are attached directly to the main line, but are folded parallel to it so that coupling is both by direct connection and by fringing fields. Easy to use formulas are given for the exact design of band-stop filters from low-pass prototype filters and equations are given for converting from one form of filter structure to any of the other equivalent forms. The experimental results of trial designs are presented.

## I. GENERAL

VARIOUS TECHNIQUES for the exact synthesis of microwave filters have existed for some time.<sup>1-5</sup>

In many cases, these procedures have involved the synthesis of special transfer functions and then the determination of the filter elements from the transfer function. Although these procedures are mathematically very elegant, they have found little actual application in microwave engineering because of the very tedious nature of the design process. However, one procedure, described by Ozaki and Ishii,<sup>4</sup> utilizes Kuroda's transformation<sup>4</sup> applied in a simple way to lumped-element, low-pass filters in order to design a certain type of transmission-line filter (which happens to be useful as a practical band-stop filter). In this case, the use of a low-pass prototype along with Kuroda's transformation makes it possible to avoid most of the complexity inherent in many of the exact procedures.

Though the procedure of Ozaki and Ishii mentioned above<sup>4</sup> was described in mathematical form quite some time ago, no investigation of its practical nature appears to have been made. In this study, the practical useful-

\* Received May 27, 1963; revised manuscript received July 31, 1963. This work was supported by the U. S. Army Electronics Research and Development Laboratory, Fort Monmouth, N. J., as part of Contract DA 36-039 SC-87398.

† Stanford Research Institute, Menlo Park, Calif.

<sup>1</sup> P. I. Richards, "Resistor-transmission-line circuits," PROC. IRE, vol. 36, pp. 217-220; February, 1948.

<sup>2</sup> H. Ozaki and J. Ishii, "Synthesis of transmission-line networks and the design of UHF filters," IRE TRANS. ON CIRCUIT THEORY, vol. CT-2, pp. 325-336; December, 1955.

<sup>3</sup> E. M. T. Jones, "Synthesis of wide-band microwave filters to have prescribed insertion loss," IRE 1956 NATIONAL CONVENTION RECORD, pt. 5, pp. 119-128.

<sup>4</sup> H. Ozaki and J. Ishii, "Synthesis of a class of strip-line filters," IRE TRANS. ON CIRCUIT THEORY, vol. CT-5, pp. 104-109; June, 1958.

<sup>5</sup> A. I. Grayzel, "A synthesis procedure for transmission line networks," IRE TRANS. ON CIRCUIT THEORY, vol. CT-5, pp. 172-181; September, 1958.

ness of this procedure as applied to band-stop filter design has been verified.<sup>6-8</sup> In addition, tables of design equations have been prepared to make the results as easy as possible to use. With the aid of these tables, a designer can obtain the filter designs he requires with a minimum of computational effort and without having to go into the theory of how the equations were derived. However, the theory is discussed in Section VI.

In Section II, there is a table of transmission-line filter formulas for filters with from one to five stubs, which are well-suited to band-stop filter design. The formulas have been derived by means of these new techniques. Each filter consists of either a tandem array of quarter-wavelength-long open-circuited transmission line shunt stubs (referred to stop-band center frequency  $\omega_0$ ) connected by quarter-wavelength-long transmission lines, or its dual in which open-circuited shunt stubs are replaced by short-circuited series stubs. The shunt stub arrangement, called a basic type band-stop filter in this paper, is suitable for both balanced and unbalanced transmission-line filters operating in the TEM mode while the series stub arrangement is preferred for waveguide filters.

The characteristic impedance of each transmission-line section of the filter can be obtained by direct substitution of the element values of a low-pass ladder prototype filter into the formulas. The resulting band-stop filter response will have the same properties as that of the prototype (i.e., Chebyshev ripples, etc.). An example of a three-resonator filter design is worked out and theoretical and measured results are given.

There is no theoretical limitation on the number of  $\lambda_0/4$  sections (so long as the number is odd) that can be used to separate each stub (or resonator) from its immediate neighbors and, in the case of waveguide filters, it has been found to be desirable to separate the stubs by  $3\lambda_0/4$  in order to avoid undesirable interaction effects because of the fringing fields in the vicinity of the resonator stubs. In Section III, design equations are

<sup>6</sup> B. M. Schiffman, P. S. Carter, Jr., and G. L. Matthaei, "Microwave Filters and Coupling Structures," Stanford Research Institute Menlo Park, Calif., Quarterly Progress Rept. 7, Section II, SRI Project 3527, Contract DA 36-039 SC-87398; October, 1962.

<sup>7</sup> G. L. Matthaei, Leo Young, and E. M. T. Jones, "Design of Microwave Filters, Impedance Matching Networks, and Coupling Structures," Stanford Research Institute, Menlo Park, Calif., SRI Project 3527, Contract DA 36-039 SC-87398; January, 1963. See Sec. 12.09.

<sup>8</sup> G. L. Matthaei, B. M. Schiffman, E. G. Cristal and L. A. Robinson, "Microwave Filters and Coupling Structures," Stanford Research Institute, Menlo Park, Calif., Final Rept., Sec. IV, SRI Project 3527, Contract DA 36-039 SC-87398; February, 1963.

given for filters having  $3\lambda_0/4$  spacings between resonators, for the cases of two and three resonators.

Although these basic stub forms of band-stop filters are conceptually simple and easy to design, they are not suitable for filters requiring very narrow stop-bands. The reason for this limitation is the difficulty of constructing stub lines with the high value of characteristic impedance required in such a filter. To overcome this difficulty and also to allow greater freedom to the designer in general, other configurations of the band-stop filter are described here, together with design equations for converting the basic configuration to one of the newer types.

Two of these newer forms, both of which employ parallel-coupled lines, are completely consonant with the exact design procedure. A filter section of the first type, which is described in Section IV, has a stub resonator that is open-circuited on one end and short-circuited on the other<sup>8,9</sup> and is separate from the main line. This type is particularly useful for filters with very narrow stop-bands, because the stop-band width is essentially a function of the degree of coupling between the stub and main line.

The second type of filter employing coupled lines is suitable for wide bandwidths. This type of filter, described in Section V, is similar to the first except that the stub is open-circuited on one end and directly connected to the main line at the other end.<sup>8</sup> Because of its form, it is called a spur-line type of filter here. In both types, there is electromagnetic coupling between the stub and the main line along the full length of the stub.

In each of the two described cases employing coupled lines, it is required that a basic band-stop filter be designed as a first step. Then, from this basic circuit (or its dual), one of the three alternative forms can be designed with the aid of the given equations.

In Section VI, the derivation of the formulas is fully described. The designer can thereby extend the table of formulas to greater values of  $n$ , which is the number of reactive elements in the prototype filter, and also derive formulas for transmission-line filters having connecting lines any desired odd number of quarter wavelengths long.

## II. DESIGN FORMULAS AND THEIR USE

The relationship of the low-pass prototype response to that of the basic transmission-line filter is illustrated in Fig. 1 and Fig. 2. One notes that the transmission-line filter response has, in addition to a low pass band, an infinite number of higher pass bands, each centered on an even multiple of the design frequency  $\omega_0$ . The peaks of attenuation at  $\omega_0$ ,  $3\omega_0$ , etc., each have a multiple-order pole of attenuation, the order of the pole being

<sup>9</sup> E. M. T. Jones and J. T. Bolljahn, "Coupled-strip-transmission-line filters and directional couplers," IRE TRANS. ON MICROWAVE THEORY AND TECHNIQUES, vol. 4, pp. 75-81; April, 1956.

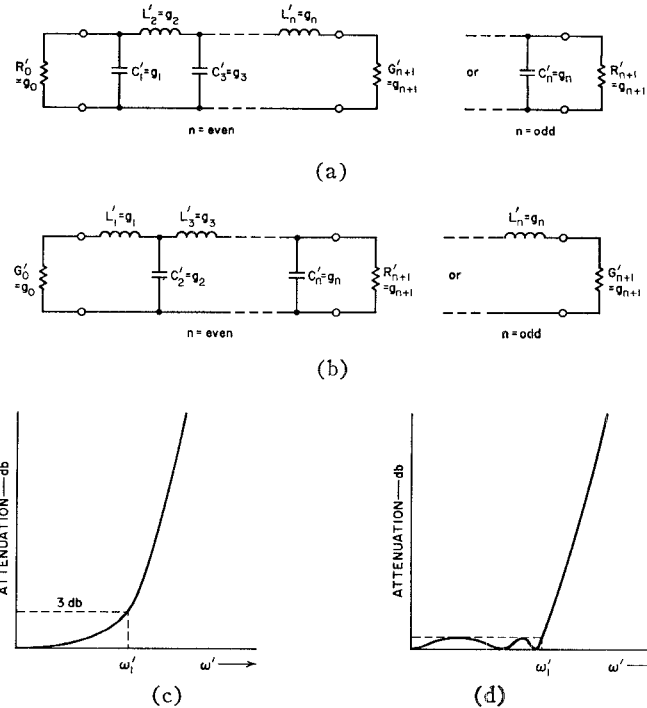


Fig. 1—Low-pass prototype filter. (a), (b) Four basic circuit types defining the parameters  $g_0, g_1, \dots, g_{n+1}$ . (c), (d) Maximally flat and equiripple characteristics defining the band-edge  $\omega_1^1$ .

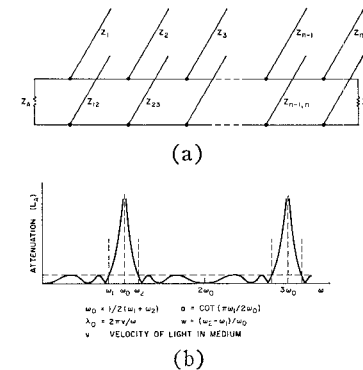


Fig. 2—Band-stop filter. (a) Transmission-line filter derived from  $n$ -element low-pass prototype. (b) Equiripple characteristic defining center frequency  $\omega_0$ , parameter  $a$  and stop-band fractional bandwidth. All stubs and connecting lines are  $\lambda_0/4$  long.

equal to the number  $n$  of resonators used in the band-stop filter structure (which is equal to the number of reactive elements in the low-pass prototype).

Table I relates specific frequencies of the lumped-element low-pass prototype filter in the  $\omega'$ -plane to corresponding frequencies of the transmission-line filter in the  $\omega$ -plane. The mapping function which maps the  $\omega'$ -plane into the  $\omega$ -plane is also given in Table I. Two of the three critical frequencies of the low-pass prototype  $\omega'=0$  and  $\omega'=\infty$  are fixed and the third  $\omega_1'$  is the cutoff frequency of the prototype filter.

The formulas for transforming the prototype networks of Fig. 1 to the transmission-line network of Fig. 2 (or to the dual of that network) are given in Table II.

TABLE I

DEFINITION OF PARAMETERS AND CORRESPONDENCE OF CRITICAL FREQUENCIES IN  $\omega'$ -PLANE AND  $\omega$ -PLANE

| Transformation                           |   |
|--|---|
|  | $\omega' = \Lambda \tan \left( \frac{\pi}{2} \frac{\omega}{\omega_0} \right)$ |
| Definition of Parameters                 |   |
| $\omega'$                                | Prototype frequency variable  |
| $\omega$                                 | Transmission line filter frequency variable                                   |
| $\Lambda$                                | $a\omega_1'$  |
| $a$                                      | $\cot \left( \frac{\pi}{2} \frac{\omega_1}{\omega_0} \right)$                 |
| Frequency Correspondences                |   |
| $\omega'$                                | $\omega$  |
| 0  | 0   |
| $\omega_1'$ ( $0 < \omega_1' < \infty$ ) | $m\omega_0 \pm \omega_1$ ( $m$ even)  |
| $\infty$                                 | $n\omega_0$ ( $n$ odd)  |

To use Table II, one must determine the following quantities:

- 1) The left-hand terminating impedance  $Z_A$  for the shunt stub type filter or  $Y_A$  of the series stub type filter (dual case),
- 2) The element values of the prototype circuit  $g_j$  ( $j=0$  to  $n+1$ ) and the cutoff frequency  $\omega_1'$  of the prototype,
- 3) The stop-band center frequency  $\omega_0$ ,
- 4) The bandwidth parameter  $a$ .

Numbers 1) and 3) are arbitrary and 2) may be obtained from tables (see Weinberg<sup>10,11</sup> or Matthaei, Young and Jones<sup>12</sup>) or from any suitable prototype ladder circuit consisting of alternate series inductors and shunt capacitors. The element values  $g_j$  ( $j=1$  to  $n$ ) are the inductance of the series inductors in henries and the capacitance of the shunt capacitors in farads. The first and last elements  $g_0$  and  $g_{n+1}$  are the prototype filter terminations given as resistance in ohms or conductance in mhos according to Fig. 1. Number 4) is calculated from the formula

$$a = \cot \left( \frac{\pi}{2} \frac{\omega_1}{\omega_0} \right) \quad (1)$$

<sup>10</sup> L. Weinberg, "Network Design by Use of Modern Synthesis Techniques and Tables," Hughes Aircraft Company, Research Laboratories, Culver City, Calif., Tech. Memo 427; April, 1956. Also *Proc. of the Natl. Electronics Conf.*, vol. 12, 1956.

<sup>11</sup> L. Weinberg, "Additional tables for design of optimum ladder networks," *J. Franklin Inst.*, vol. 264, pt. I, p. 7, July, 1957; and pt. II, p. 127, August, 1957.

<sup>12</sup> G. L. Matthaei, L. Young, and E. M. T. Jones, *op. cit.*, ch. IV.

TABLE II

EXACT EQUATIONS FOR BAND-STOP FILTERS WITH  $\lambda_0/4$  SPACING BETWEEN STUBS

The filter structure is as shown in Fig. 2. For the dual case having short-circuited series stubs, replace all impedances in the equations below by corresponding admittances.

$n$  = number of stubs  
 $Z_A, Z_B$  = terminating impedances  
 $Z_j$  ( $j=1$  to  $n$ ) = impedances of open-circuited shunt stubs  
 $Z_{j-1,j}$  ( $j=2$  to  $n$ ) = connecting line impedances  
 $g_j$  = values of the elements of the low-pass prototype network as defined in Fig. 1.  
 $\Lambda = \omega_1' a$  where  $\omega_1'$  = low-pass prototype cutoff frequency and  $a$  = bandwidth parameter defined in (1).  
(In all cases the left terminating impedance  $Z_A$  is arbitrary.)

Case of  $n=1$ 

$$Z_1 = \frac{Z_A}{\Lambda g_0 g_1}, \quad Z_B = \frac{Z_A g_2}{g_0}.$$

Case of  $n=2$ 

$$Z_1 = Z_A \left( 1 + \frac{1}{\Lambda g_0 g_1} \right), \quad Z_{12} = Z_A (1 + \Lambda g_0 g_1),$$

$$Z_2 = \frac{Z_A g_0}{\Lambda g_2}, \quad Z_B = Z_A g_0 g_3.$$

Case of  $n=3$  $Z_1, Z_{12}$  and  $Z_2$  — same formulas as Case  $n=2$ .

$$Z_3 = \frac{Z_A g_0}{g_4} \left( 1 + \frac{1}{\Lambda g_3 g_4} \right), \quad Z_{23} = \frac{Z_A g_0}{g_4} (1 + \Lambda g_3 g_4),$$

$$Z_B = \frac{Z_A g_0}{g_4}.$$

Case of  $n=4$ 

$$Z_1 = Z_A \left( 2 + \frac{1}{\Lambda g_0 g_1} \right), \quad Z_{12} = Z_A \left( \frac{1 + 2\Lambda g_0 g_1}{1 + \Lambda g_0 g_1} \right),$$

$$Z_2 = Z_A \left( \frac{1}{1 + \Lambda g_0 g_1} + \frac{g_0}{\Lambda g_2 (1 + \Lambda g_0 g_1)^2} \right), \quad Z_{23} = \frac{Z_A}{g_0} \left( \Lambda g_2 + \frac{g_0}{1 + \Lambda g_0 g_1} \right),$$

$$Z_3 = \frac{Z_A}{\Lambda g_0 g_3}, \quad Z_{34} = \frac{Z_A}{g_0 g_5} (1 + \Lambda g_4 g_5),$$

$$Z_4 = \frac{Z_A}{g_0 g_5} \left( 1 + \frac{1}{\Lambda g_4 g_5} \right), \quad Z_B = \frac{Z_A}{g_0 g_5}.$$

Case of  $n=5$  $Z_1, Z_{12}, Z_2, Z_{23}, Z_3$  — same formulas as Case  $n=4$ .

$$Z_4 = \frac{Z_A}{g_0} \left( \frac{1}{1 + \Lambda g_5 g_6} + \frac{g_6}{\Lambda g_4 (1 + \Lambda g_4 g_5)^2} \right), \quad Z_{34} = -\frac{Z_A}{g_0} \left( \Lambda g_4 + \frac{g_6}{1 + \Lambda g_5 g_6} \right),$$

$$Z_5 = \frac{Z_A g_6}{g_0} \left( 2 + \frac{1}{\Lambda g_5 g_6} \right), \quad Z_{45} = \frac{Z_A g_6}{g_0} \left( \frac{1 + 2\Lambda g_5 g_6}{1 + \Lambda g_5 g_6} \right),$$

$$Z_B = \frac{Z_A g_6}{g_0}.$$

where  $\omega_1$  is the lower cutoff frequency of the transmission-line filter which corresponds with  $\omega_1'$  of the low-pass prototype filter.

The following example will illustrate the use of the design formulas and the practical realization of a strip-line filter employing open-circuited stubs. A band-stop filter having 50- $\Omega$  input impedance, 0.1-db pass-band ripple and 60 per cent stop-band bandwidth is desired and a three-stub design is chosen. The center of the stop band is to be 1.6 Gc. The prototype element values (obtained from Table 4.05-2(a) in Matthaei, Young and Jones<sup>12</sup> or Weinberg<sup>10,11</sup>) are  $g_0 = g_4 = 1$ ,  $g_1 = g_3 = 1.0315$

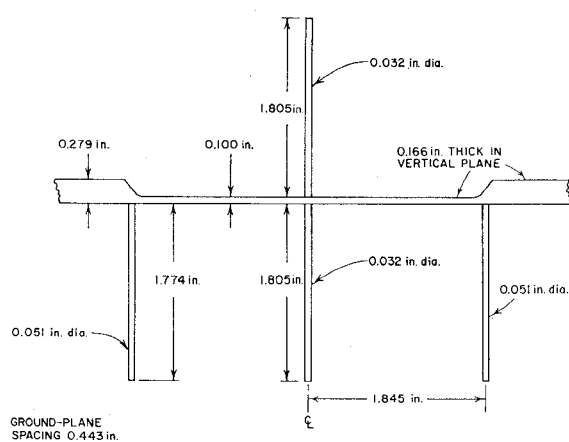


Fig. 3—A strip-line wide-stop-band filter.

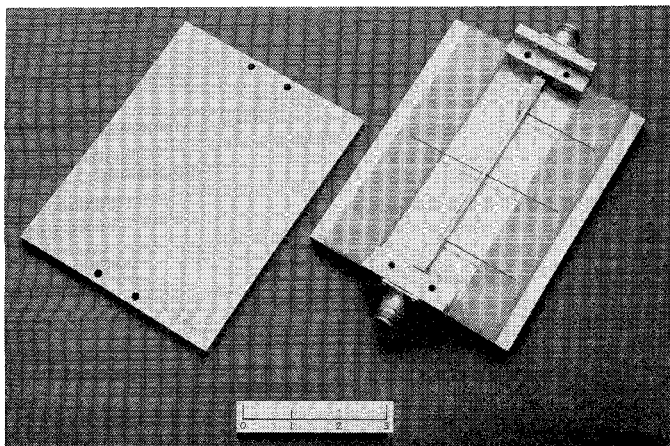


Fig. 4—Photograph of the strip-line wide-stop-band filter.

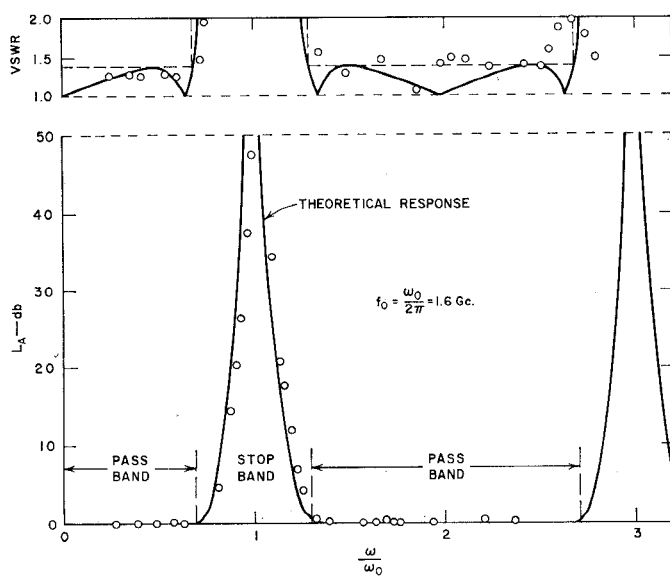


Fig. 5—Computed and measured performance of the wide-stop-band filter in Fig. 4.

and  $g_2 = 1.1474$ . The quantity  $\Lambda = \omega_1' a$  is next computed. For the prototype chosen,  $\omega_1' = 1$  radian per second. From the fractional bandwidth  $w = 0.6$ , as defined in Fig. 2, we obtain  $\omega_1/\omega_0 = 0.7$ , and the bandwidth parameter  $a = \cot(\pi\omega_1/2\omega_0)$  is found to be 0.50953, thus  $\Lambda = 0.50953$ . Now using  $Z_A = 50 \Omega$  as the source impedance, we calculate each stub and connecting-line impedance. Since  $n$  is odd and the prototype design is symmetrical, the design formulas here yield a symmetrical transmission line design so that the right-hand terminating impedance  $Z_B = 50 \Omega$ . The stub impedances are calculated from the design formulas of Table II for  $n = 3$  to be  $Z_1 = Z_3 = 145.1 \Omega$  and  $Z_2 = 85.5 \Omega$ . The two connecting-line impedances are  $Z_{12} = Z_{23} = 76.3 \Omega$ . Each stub and connecting line is then made one-quarter wavelength long at  $\omega_0$ .

A filter based on the foregoing design was fabricated in strip transmission line. With air as the dielectric,  $\lambda_0/4$  is found to be 1.845 inches. The center stub was replaced by two parallel stubs of twice the impedance, *i.e.*, with  $Z = 2Z_2 = 171.0 \Omega$ , in order to minimize the junction size and thereby reduce junction effect. The essential dimensions are given in Fig. 3. The stub lengths were reduced by an amount slightly more than one diameter to allow for fringing capacitance at the ends of the stubs.

A photograph of the filter is shown in Fig. 4. The rectangular center-conductor dimensions were obtained from Fig. 6 in Bates<sup>13</sup> and the cylindrical stubs were designed with the aid of the following approximate formula for the impedance of a round conductor between parallel planes:

$$Z_0 = \frac{138}{\sqrt{\epsilon}} \log_{10} \frac{4b}{\pi d} \quad (2)$$

where  $d$  is the diameter of center conductor and  $b$  is the plate-to-plate spacing.

The computed and measured performance of this filter is given in Fig. 5. The measured results agree well with the theoretical predictions over a rather broad band; however, some improvement could have been obtained by using tuning screws to make the stubs resonate precisely at the desired stop-band center frequency.

### III. FORMULAS FOR FILTERS WITH $3\lambda_0/4$ SPACING BETWEEN RESONATORS

In the case of waveguide band-stop filters, the dual form of filter to that in Fig. 2 a) (*i.e.*, the form using short-circuited series stubs and connecting lines) is usually preferable. If the bandwidth of the filter is very narrow, the impedances of the series stubs will be very low, so that it is desirable to replace the stubs with half-wavelength cavity resonators and coupling irises<sup>6</sup>

<sup>13</sup> R. H. Bates, "The characteristic impedance of shielded slab lines," IRE TRANS. ON MICROWAVE THEORY AND TECHNIQUES, pp. 28-33; January, 1956.

TABLE III

EXACT EQUATIONS FOR BAND-STOP FILTERS WITH  $3\lambda_0/4$  SPACING BETWEEN STUBS OR RESONATOR IRISES

The filter structure is of the form in Fig. 6 (a). For the dual case in Fig. 6 (b) replace all admittances in the equations below with corresponding impedances.

$n$  = number of stubs

$Y_A, Y_B$  = terminating admittances

$Y_j$  ( $j = 1$  to  $n$ ) = admittances of short-circuited series stubs

$(Y_{j-1,j})_k$  = admittance of  $k$ th ( $k = 1, 2$  or  $3$ ) connecting line from the left between stubs  $j-1$  and  $j$

$g_i$  = values of the elements of the low-pass prototype network as defined in Fig. 1

$\Lambda = \omega_1' a$  where  $\omega_1'$  = low-pass cutoff frequency and  $a$  = bandwidth parameter defined in (1).

(In all cases the left terminating impedance is arbitrary)

Case of  $n = 2$

$$Y_1 = Y_A \left( 1 + \frac{1}{\Lambda g_0 g_1} \right), \quad (Y_{12})_1 = Y_A (1 + \Lambda g_0 g_1),$$

$$Y_2 = Y_A \frac{g_0}{\Lambda g_2} (1 + 2\Lambda g_2 g_3), \quad (Y_{12})_2 = Y_A g_0 g_3 \left( \frac{1}{1 + \Lambda g_2 g_3} \right),$$

$$Y_B = Y_A g_0 g_3, \quad (Y_{12})_3 = Y_A g_0 g_3 \left( \frac{1 + 2\Lambda g_2 g_3}{1 + \Lambda g_2 g_3} \right).$$

Case of  $n = 3$

$$Y_1 = Y_A \left( 3 + \frac{1}{\Lambda g_0 g_1} \right), \quad (Y_{12})_1 = Y_A \left( \frac{1 + 3\Lambda g_0 g_1}{1 + 2\Lambda g_0 g_1} \right),$$

$$(Y_{12})_2 = Y_A \left( \frac{1 + \Lambda g_0 g_1}{1 + 2\Lambda g_0 g_1} \right),$$

$$Y_2 = Y_A \frac{g_0}{\Lambda g_2}, \quad (Y_{12})_3 = Y_A (1 + \Lambda g_0 g_1),$$

$$(Y_{23})_1 = Y_A \frac{g_0}{g_4} (1 + \Lambda g_3 g_4),$$

$$Y_3 = Y_A \frac{g_0}{g_4} \left( 3 + \frac{1}{\Lambda g_3 g_4} \right), \quad (Y_{23})_2 = Y_A \frac{g_0}{g_4} \left( \frac{1 + \Lambda g_3 g_4}{1 + 2\Lambda g_3 g_4} \right),$$

$$Y_B = Y_A \frac{g_0}{g_4}, \quad (Y_{23})_3 = Y_A \frac{g_0}{g_4} \left( \frac{1 + 3\Lambda g_3 g_4}{1 + 2\Lambda g_3 g_4} \right).$$

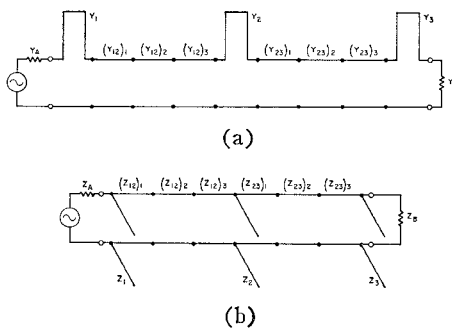


Fig. 6—Band-stop filters with  $3\lambda_0/4$  spacing between  $\lambda_0/4$  stubs.

with the coupling-iris sizes adjusted to give the required resonator slope parameters.<sup>14,6</sup> This introduces an approximation into the design, but the results are generally more accurate than is achieved by use of the approximate procedure described in Young, Matthaei and Jones.<sup>14</sup>

<sup>14</sup> L. Young, G. L. Matthaei, and E. M. T. Jones, "Microwave band-stop filters with narrow stop bands," IRE TRANS. ON MICROWAVE THEORY AND TECHNIQUES, vol. 10, pp. 416-427; November, 1962.

Previous experience with waveguide band-stop filters has shown that it is desirable to separate the resonators by  $3\lambda_0/4$  instead of  $\lambda_0/4$  in order to avoid interaction effects due to the fringing fields in the vicinity of the coupling irises. For this reason, equations for the exact design of stub filters having  $3\lambda_0/4$  spacings between stubs were prepared in this study. It is expected that these equations will be used as the basis for the design of waveguide band-stop filters by replacing the stubs called for by the equations with iris-coupled resonators as mentioned above, and by replacing  $\lambda_0$  by  $\lambda_{\theta 0}$ .

Table III presents equations for the design of filters with series-connected stubs with  $3\lambda_0/4$  spacings between stubs, for the cases of  $n = 2$  and  $n = 3$  stubs. The configuration under consideration is shown in Fig. 6 a). However, by duality, the same equations can be made to apply also to the structure in Fig. 6 b) by simply redefining all of the admittances in Table III as impedances. The resonator susceptance slope parameters<sup>14</sup> for the series stubs in Fig. 6 a) are given by

$$b_j = \frac{\pi}{4} Y_j. \quad (3)$$

Having the admittances of the connecting line sections and also the slope parameters required for the various resonators, the designer can carry out the remainder of the waveguide filter design using the procedure that was discussed previously.<sup>14</sup>

#### IV. PARALLEL-COUPLED-RESONATOR FILTER

A single section of the parallel-coupled-resonator type filter suitable for narrow stop-bands is shown in Fig. 7. Also shown is the corresponding portion of the basic stub form of filter and design equations that enable the basic filter to be converted, section by section, into the parallel-coupled type. The coupled lines are completely specified by their even- and odd-mode impedances  $Z_{oe}^a, Z_{oe}^b, Z_{oo}^a, Z_{oo}^b$  (or their odd- and even-mode admittances).<sup>4,9</sup> The superscripts  $a$  and  $b$  pertain to lines  $a$  and  $b$  in Fig. 7.

Before the formulas can be applied, it is necessary to partition the basic filter, shown in Fig. 2 a), so that each section has one length of connecting line and one stub, according to Fig. 7. Since there are more stubs (one more) than connecting lines, one quarter-wavelength section of connecting line must be inserted between the filter and one of the terminations. The characteristic impedance of the inserted section must, of course, equal the terminating impedance; although the filter amplitude response will be unaltered by this change, some time delay will be added to the signal.

The conversion formulas yield values for the distributed capacitances of the coupled lines as illustrated in Fig. 8. These distributed capacitances  $C_a, C_b$  and  $C_{ab}$ , pertaining to lines  $a$  and  $b$  shown in the form of a general  $\pi$ -network, are directly related to the even- and odd-mode admittances (or impedances) of the coupled

Unsymmetrical Case:  $\begin{cases} C_a = \frac{\eta_0}{\epsilon \sqrt{\epsilon_r}} (Y_{12} + Y_2) - \frac{C_{ab}}{\epsilon} \\ C_b = \frac{\sqrt{\epsilon_r}}{\epsilon} \left( \frac{C_{ab}}{\epsilon} \right)^2 - \frac{C_{ab}}{\epsilon} \end{cases}$  with  $C_{ab}$  arbitrary (see text)

Symmetrical Case:  $\begin{cases} C_a = C_b = \frac{\eta_0}{\epsilon \sqrt{\epsilon_r}} [Y_{12} + Y_2] \\ C_{ab} = \frac{\eta_0}{\epsilon \sqrt{\epsilon_r}} \sqrt{Y_2(Y_{12} + Y_2)} \end{cases}$

Fig. 7—Parallel-coupled transmission-line section and equivalent section of basic filter.

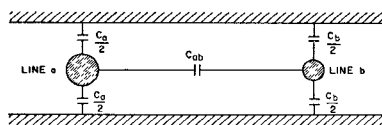


Fig. 8—An unsymmetrical pair of parallel-coupled lines;  $C_a$ ,  $C_{ab}$  and  $C_b$  are line capacitances per unit length.

lines.<sup>8,9</sup> The formulas give distributed capacitances directly because these quantities are most useful in designing coupled-rectangular-bar strip lines. The coupled lines may be symmetrical ( $C_a = C_b$ ) or unsymmetrical ( $C_a \neq C_b$ ).

If it is desired that the coupled lines be symmetrical, the right set of equations of Fig. 7 is used. If the coupled lines are made unsymmetrical, the value of  $C_{ab}$  is arbitrarily chosen (subject to the condition that positive values are obtained for  $C_a$  and  $C_b$ ) and the left set of equations is used.

The relationship of the capacitances of the  $\pi$ -network of Fig. 8 to the component capacitances (*i.e.*, parallel-plate and fringing capacitances) of parallel-coupled rectangular bars is easily seen in Fig. 9. Since the capacitances  $C_a$  and  $C_b$  are not necessarily equal, the two coupled lines of each section need not be identical in cross section. However, as explained below, by restricting the heights so that the two rectangular bars are equal and further limiting the strip-line proportions, the coupled lines of both the symmetrical and unsymmetrical type can be easily designed with the aid of Getsinger's graphs of fringing capacitances.<sup>15</sup>

Getsinger<sup>15</sup> has derived equations for the fringing capacitances  $C_{fe}$ ,  $C_{fo}$  and  $C_f$  of rectangular bars shown in Fig. 9 and has prepared convenient charts which relate  $C_{fe}/\epsilon$ ,  $C_{fo}/\epsilon$ , and  $C_f/\epsilon$  to rectangular-bar strip-line dimensions. Here  $\epsilon$  is the dielectric constant of the medium of propagation, so that the above ratios are dimensionless and of moderate size. Getsinger gives equations for the design of symmetrical, parallel-coupled, rectangular strip-lines and here we adapt his

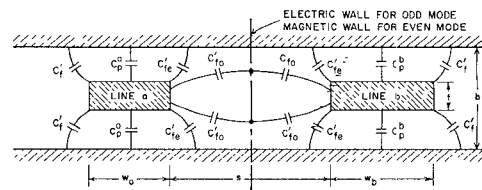


Fig. 9—Cross section of unsymmetrical, rectangular-bar parallel-coupled lines.

equations to fit the unsymmetrical, as well as the symmetrical, case.

Note that the shape of the strip lines in Fig. 9 is specified in terms of the dimensions  $t$ ,  $b$ ,  $s$ ,  $w_a$  and  $w_b$ . To design a pair of lines such as those in Fig. 9, to have odd- and even-mode admittances or impedances as determined implicitly by the calculated values of  $C_a/\epsilon$ ,  $C_{ab}/\epsilon$  and  $C_b/\epsilon$ , first select a convenient value for  $t/b$ . Then, noting that

$$\frac{\Delta C}{\epsilon} = \frac{C_{ab}}{\epsilon}, \quad (4)$$

use Getsinger's chart<sup>15</sup> of  $\Delta C/\epsilon$  and  $C_{fe}'$  vs  $s/b$  to determine  $s/b$  and also  $C_{fe}'/\epsilon$ . Using  $t/b$  and Getsinger's chart of  $C_f'$  vs  $t/b$ , determine  $C_f'/\epsilon$  and then compute

$$\frac{w_a}{b} = \frac{1}{2} \left( 1 - \frac{t}{b} \right) \left[ \frac{1}{2} \left( \frac{C_a}{\epsilon} \right) - \frac{C_{fe}'}{\epsilon} - \frac{C_f'}{\epsilon} \right], \quad (5)$$

$$\frac{w_b}{b} = \frac{1}{2} \left( 1 - \frac{t}{b} \right) \left[ \frac{1}{2} \left( \frac{C_b}{\epsilon} \right) - \frac{C_{fe}'}{\epsilon} - \frac{C_f'}{\epsilon} \right]. \quad (6)$$

When the ground plane spacing  $b$  is specified, the required bar widths  $w_a$  and  $w_b$  are determined. This procedure also works for the thin-strip case where  $t/b=0$ . If either  $w_a/b$  or  $w_b/b$  is less than  $0.35(1-t/b)$ , the width of the bar should be corrected using the approximate formula

$$\frac{w'}{b} = \frac{0.07 \left( 1 - \frac{t}{b} \right) + \frac{w}{b}}{1.20}, \quad (7)$$

providing that  $0.1 < (w'/b)/(1-t/b) < 0.35$ . In (5), (6) and (7),  $w$  is the uncorrected bar width and  $w'$  is the corrected width. The need for this correction arises because of the interaction of the fringing fields at opposite sides of a bar, which will occur when a bar is relatively narrow.

The strip-line filter shown in Fig. 10 was designed by the methods outlined here. The stop-band center frequency is 1.6 Gc. The prototype filter has two elements and a maximally flat response. The prototype element values are  $g_0=g_3=1$ ,  $g_1=g_2=1.414$  and  $\omega_1'=1$ . The characteristic impedance values of the basic two-stub filter, designed with the aid of the formulas in Table II for a 5 per cent width of the stop-band (between 3-db points) and 50- $\Omega$  terminations, are  $Z_1=949.9 \Omega$  and  $Z_2=899.9 \Omega$  for the shunt-stub characteristic impedances and  $Z_{12}=52.8 \Omega$  for the connecting-line imped-

<sup>15</sup> W. J. Getsinger, "Coupled rectangular bars between parallel plates," IRE TRANS. ON MICROWAVE THEORY AND TECHNIQUES, vol. 10, pp. 65-72; January, 1962.

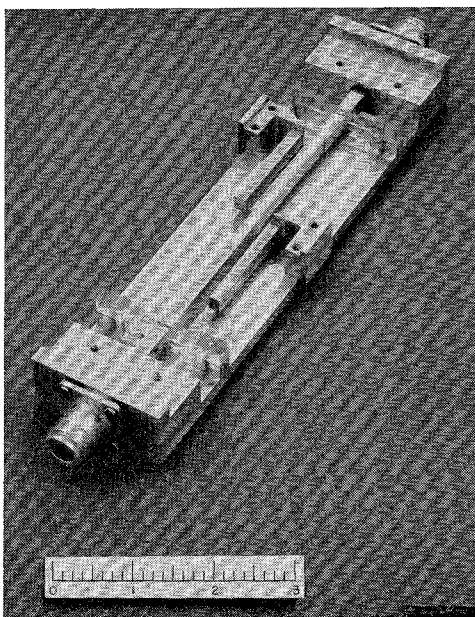


Fig. 10—A parallel-coupled-line, narrow-band filter with cover plate removed.

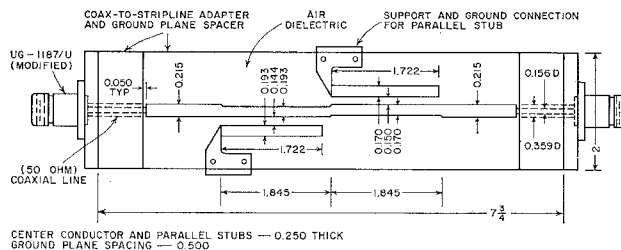
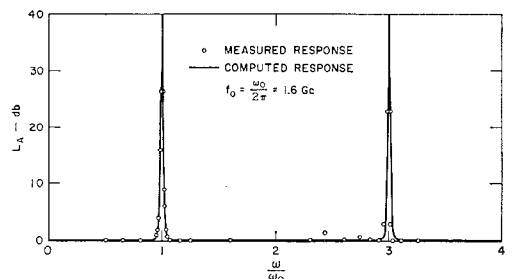


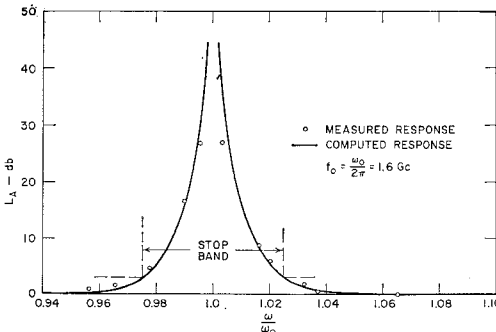
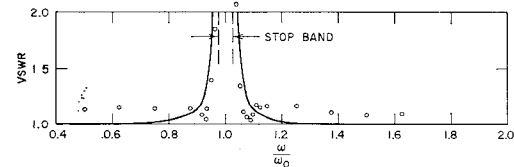
Fig. 11—Sketch of a parallel-coupled-line, narrow-band filter with cover plate removed, showing dimensions in inches.

ance. A quarter-wavelength section of  $50\Omega$  impedance line was inserted between Stub 2 and the  $50\Omega$  termination, thus yielding two complete  $L$ -sections ready to convert to two sections of parallel-coupled lines. The symmetrical type of coupled-line construction was chosen for the filter. The values of distributed capacitance (normalized to the permittivity of the medium) were then calculated with the aid of the formulas of Fig. 7 and found to be 1) for Section 1 (corresponding to Stub 1 and its connecting line),  $C_a/\epsilon = C_b/\epsilon = 5.80$  and  $C_{ab}/\epsilon = 1.73$  and 2) for Section 2 (corresponding to Stub 2 and the added  $50\Omega$  section),  $C_a/\epsilon = C_b/\epsilon = 6.12$  and  $C_{ab}/\epsilon = 1.82$ . With the aid of Getsinger's graphs<sup>15</sup> the strip-line dimensions shown in Fig. 11 were obtained.

Each parallel-coupled resonator and its grounding wedge were milled from a solid piece of aluminum. Each resonator length is slightly less than  $\lambda_0/4$ , as determined experimentally, to allow for fringing capacity. The measured and computed responses of the filter are shown in Fig. 12. The stop-band center frequency was found, after the final adjustments of the lengths of the resonators, to be  $f_0 = 1.608$  Gc and the curves of Fig. 12 are plotted with frequency normalized to  $f_0$ . The measured attenuation loss points are seen to be in excellent



(a)



(b)

Fig. 12—Measured and computed response of filter in Fig. 11.

agreement with the computed values over a very wide frequency range, even including the second stop-band at  $3f_0$ .

## V. SPUR-LINE TYPE OF FILTER

A second type of band-stop filter section employing coupled lines is shown together with its design formulas in Fig. 13. Because of the direct connection (and the resulting strong coupling) of the stub to the line, this type of filter is similar to the basic type. In the limit, as the coupled lines are separated until there is very little distributed coupling, the structure becomes almost identical to the basic shunt-stub filter section. The spur-line type of construction is thus suitable for filters with wide stop-bands. In general, the energy stored in the resonant structure is determined mainly by the electromagnetic fields of the odd mode of propagation. This energy can be reduced and the bandwidth narrowed by reducing  $Z_{00}$ —that is, by bringing the coupled lines close together—but this process has a practical limit. Furthermore, copper losses would tend to increase and thereby reduce the maximum attainable attenuation in the stop-band.

A two-resonator spur-line-type band-stop filter was designed with the aid of the formulas of Fig. 13 for 60 per cent stop-band bandwidth and 1.6-Gc stop-band center frequency. Here again, as for the narrow-stop-band described in Section IV, symmetrical coupled

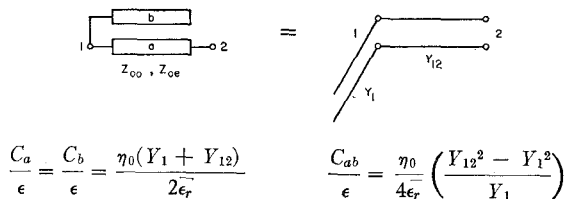


Fig. 13—Spur-line stub resonator and equivalent section of basic filter.

lines were used. The prototype circuit was chosen to have maximally flat response and its element values are, as before,  $g_0 = g_3 = 1$ ,  $g_1 = g_2 = 1.414$ , with  $\omega_1' = 1$ .

The basic filter element values were found to be  $Z_1 = 119.3 \Omega$  and  $Z_2 = 69.3 \Omega$  for the shunt stubs and  $Z_{12} = 86.05 \Omega$  for the connecting line. A quarter-wavelength section of  $50-\Omega$  line was then connected to one end of the filter so that it could be properly partitioned. The two possible circuits thus obtained and their methods of partitioning are shown in Fig. 14 a) and b). Trial paper designs based on those circuits yielded coupled rectangular bar lines of such proportions that it was feared that the discontinuities at the junctions of the two sections and main line would be large enough to badly degrade the performance. The circuit of Fig. 14 c) was found superior in this respect. This circuit, which was used in the design of the filter, was derived from the basic circuit [Fig. 2a)] as follows. First, the dual of the basic circuit was calculated by the equation

$$Z_D = \frac{Z_0^2}{Z} \quad (8)$$

where  $Z_0^2 = Z_A Z_B = (50)^2$ ,  $Z$  is the characteristic impedance of a stub or connecting line section and  $Z_D$  is the impedance of the dual of that section of line. (The dual of a shunt stub is a series short-circuited stub and the dual of a connecting line is again a connecting line.) Then, a quarter-wavelength section of  $50-\Omega$  line was added to each end of the filter and Kuroda's identity<sup>2,6</sup> was used to move the two stubs outward, each to its end of the network, and at the same time transform the series stubs back to shunt stubs with the circuit of Fig. 14c) as a result. This circuit was then partitioned so that it could be converted to a filter structure with two spur-line sections separated by a length of line of impedance  $Z_{23} = 29.1 \Omega$ . The finished strip-line filter is shown in Fig. 15. (Note that the two spurs point toward each other and the spur-to-line junctions are separated by  $3\lambda_0/4$ . An alternative realization, in which the spurs point away from each other and their connecting points are separated  $\lambda_0/4$ , could be obtained from the original circuit [Fig. 14a)] by adding a section of  $50-\Omega$  line on the right.) A sketch of the spur-line type filter with essential dimensions is given in Fig. 16. The coupled lines were designed by the method described in Section IV.

The lengths of the spurs were individually adjusted to resonate at stop-band center as follows. The gap be-

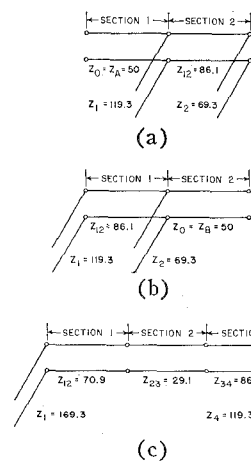


Fig. 14—Three ways of partitioning equivalent basic filters to form a spur-line filter.

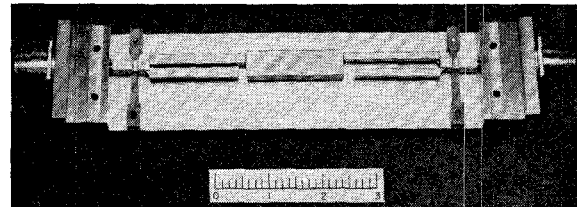


Fig. 15—A spur-line band-stop filter with cover plate removed.

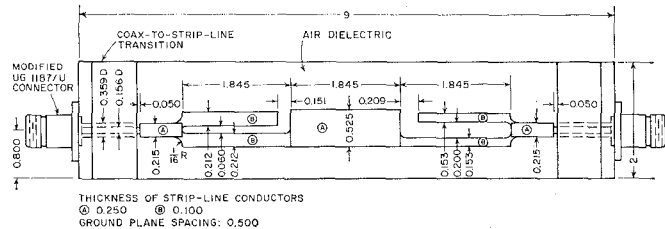


Fig. 16—Sketch of a spur-line band-stop filter with cover plate removed, showing dimensions in inches.

tween the end of one spur and the center section of the main line was bridged with adhesive aluminum foil, thereby making that spur-line section nonresonant. The frequency of maximum attenuation of the remaining resonant spur line was then measured and the unbridged spur was reduced in length about half the amount calculated to bring it to resonance at  $f_0$ , when considered to be a simple open-circuited shunt stub. (Half the calculated reduction in length was used as a safety precaution, because the capacitance of the spur end to main line is reduced at the same time and this latter value is not included in the calculation.) A few attempts brought the spur to resonance at the desired frequency and the same process was repeated for the other spur.

The measured values of attenuation loss and VSWR are shown to agree fairly well with the computed values in Fig. 17. The anomalous departure of measured values from computed values that does occur, mainly near the upper edge of the first stop-band and the lower edge of the second stop-band, may be due to the remaining discontinuities between sections, which could not be eliminated entirely.

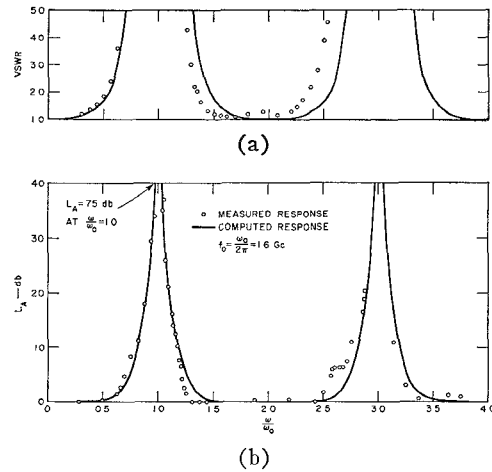


Fig. 17—Measured and computed VSWR and attenuation of filter of Fig. 15.

## VII. DERIVATION OF THE DESIGN EQUATIONS

The design procedure of this section hinges on Kuroda's identity.<sup>2,4</sup> This identity is realized in transmission line as shown in Fig. 18.<sup>6</sup> Note that this identity says that a circuit consisting of an open-circuited shunt stub and a connecting line of the same length has an exact equivalent circuit consisting of a short-circuited series stub with a connecting line at the opposite side.

Fig. 19 traces how Kuroda's identity in the transmission line form (Fig. 18) is used to relate a band-stop filter of the type in Fig. 2 a) to a low-pass prototype filter. Figure 19 a) shows a low-pass prototype filter for the case of  $n=3$  reactive elements. Applying the mapping equation of Table I to the shunt susceptances and series reactances of this filter gives

$$\omega' C'_j = C'_j \omega_1' a \tan\left(\frac{\pi}{2} \frac{\omega}{\omega_0}\right), \quad (9)$$

$$\omega' L'_j = L'_j \omega_1' a \tan\left(\frac{\pi}{2} \frac{\omega}{\omega_0}\right). \quad (10)$$

Note that the right side of (9) corresponds to the susceptance of an open-circuited stub having a characteristic admittance.

$$Y_j = C'_j \omega_1' a, \quad (11)$$

the stub being  $\lambda_0/4$  long at  $\omega_0$ . Similarly, the right side of (10) corresponds to the reactance of a short-circuited stub of characteristic impedance

$$Z_j = L'_j \omega_1' a \quad (12)$$

when the stub is  $\lambda_0/4$  long at frequency  $\omega_0$ . Thus, the shunt capacitors in the low-pass prototype become open-circuited shunt stubs in the mapped filter, while the series inductance in the prototype becomes a short-circuited series stub in the mapped filter.

Note that in the mapped filter in Fig. 19 b), the terminations seen by the reactive part of the filter are still  $R_A$  on the left and  $R_B$  on the right, even though two

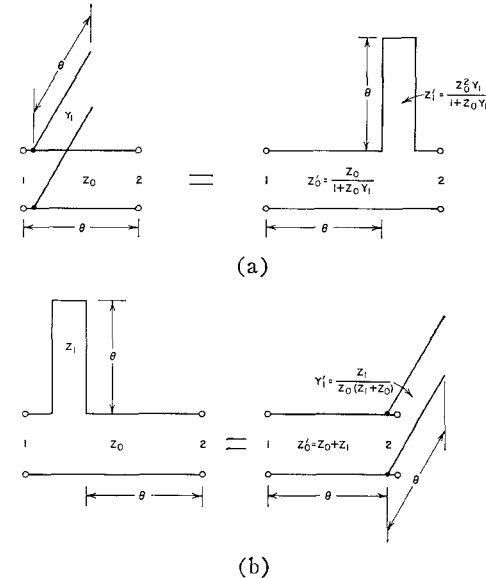


Fig. 18—Kuroda's identity in transmission-line form.

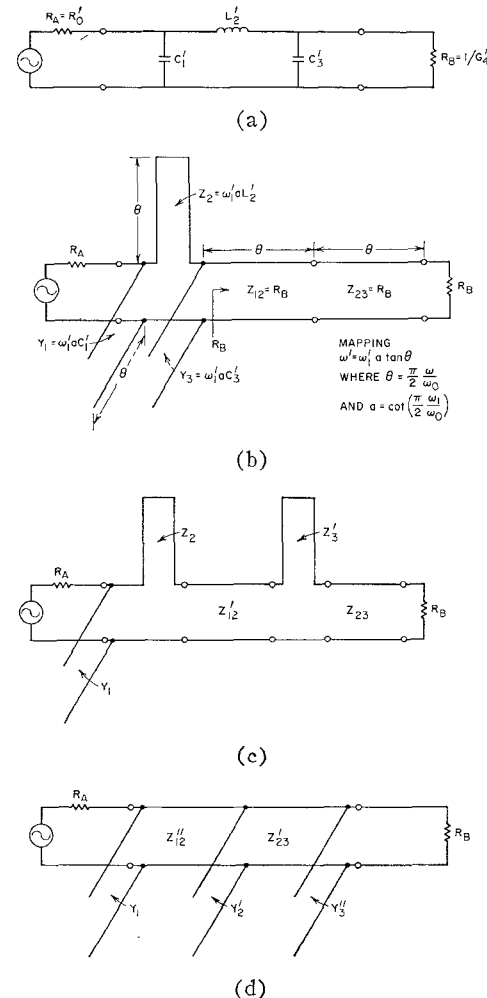


Fig. 19—Stages in the transformation of a low-pass prototype filter into a band-stop transmission-line filter. (a) Prototype. (b) Mapped prototype. (c) After applying Kuroda's identity to  $Y_3$  and  $Z_{12}$  in (b). (d) After applying Kuroda's identity to  $Z_2$  and  $Z_{12}'$  and to  $Z_{23}'$  in (c).

line sections of impedance  $Z_{12}=Z_{23}=R_B$  have been added on the right to allow the use of Kuroda's identity in the next step. Since their characteristic impedance matches that of the termination, they do not affect the attenuation characteristic of the circuit; their only effect on the response is to give some added phase shift. The circuit in Fig. 19 b) then has a response which is the desired exact mapping of the low-pass prototype response. The only trouble with the filter in Fig. 19 b) is that it contains a series stub which is difficult to construct in a shielded TEM-mode microwave structure.

The series stub in Fig. 19 b) can be eliminated by application of Kuroda's identity (Fig. 18). Applying Kuroda's identity to stub  $Y_3$  and line  $Z_{12}$  in Fig. 19 b) gives the circuit in Fig. 19 c). Then applying Kuroda's identity simultaneously to stub  $Z_2$  and line  $Z_{12}'$  and stub  $Z_3'$  and line  $Z_{23}$  in Fig. 19 c) gives the circuit in Fig. 19 d). Note that the circuit in Fig. 19 d) has exactly

the same input impedance and over-all transmission properties as the circuit in Fig. 19 b), while the circuit in Fig. 19 d) has no series stubs.

The equations in Tables II and III were derived by use of repeated applications of the procedures described above. For reasons of convenience, the equations in the tables use a somewhat different notation than does the example in Fig. 19; however, the principles used are the same. The equations in Tables II and III also provide for a shift in impedance level from that of the low-pass prototype.

#### ACKNOWLEDGMENT

R. B. Lerrick and P. R. Reznik very ably performed the measurements and adjustments on the experimental filters. The assistance of Dr. Leo Young and P. H. Omlor in adapting an existing program for computing the filter responses is most gratefully acknowledged.

## A New Microwave Measurement Technique to Characterize Diodes and an 800-Gc Cutoff Frequency Varactor at Zero Volts Bias\*

BERNARD C. DELOACH†, MEMBER, IEEE

**Summary**—A means has been found which enables one to make negligible the complicating effects of posts and shunting cartridge capacitance usually present in microwave diode circuits. This simplification permits the representation of the diode by a simple equivalent circuit and the determination of the effective diode parameters from transmission measurements. Parameters so obtained at X band (8.2 to 12.4 Gc) are compared with audio frequency bridge measurements. Measurements at M band (50–60 Gc) of a new 800-Gc cutoff frequency varactor are also described. This varactor has zero bias junction capacitance in the 0.016 pf range and spreading resistance on the order of 12  $\Omega$ . It is expected to extend the useful range of parametric devices well into the millimeter region.

### I. INTRODUCTION

THE CHARACTERISTICS of microwave diodes are usually difficult to determine at microwave frequencies. This is primarily due to so called "parasitics" arising from contacting elements, shunting cartridge capacity and supportive posts.<sup>1</sup> These can be

"calibrated" out in the standard<sup>2</sup> reflection coefficient techniques, but at high microwave frequencies where circuits become fairly lossy this method meets with considerable difficulty. This calibration can also be a strong function of temperature, which causes difficulties when one is trying to evaluate diode characteristics over a wide temperature range. In addition, this technique has the unfortunate characteristic of decreasing accuracy of measurement of diode characteristics at a given frequency, with increasing diode quality factor.

In a search for effective equivalent circuit parameters for parametric amplifiers, a technique has been developed for characterizing microwave diodes which does not have the disadvantages listed above. This technique employs the series resonance of a diode in reduced height rectangular waveguide in the form presented here, but is adaptable to other types of transmission lines such as

\* Received May 20, 1963; revised, manuscript received August 19, 1962.

† Bell Telephone Laboratories, Inc. Murray Hill, N. J.

<sup>1</sup> B. C. DeLoach, "Waveguide parametric amplifiers," *Digest of Tech. Papers of the Internat'l. Solid-State Circuits Conf.*, pp. 24–25, 1961.

<sup>2</sup> M. C. Waltz, "A technique for the measurement of microwave impedance in the junction region of a semiconductor device," *Microwave J.*, vol. 2, pp. 23–27; May, 1959.

N. Houlding, "Measurement of varactor quality," *Microwave J.*, vol. 3, pp. 40–45; January, 1960.

R. T. Harrison, "Parametric diode Q measurement," *Microwave J.*, vol. 3, pp. 43–46; May, 1960.